AIAA-91-1535-CP

Design of Algorithms for a Dispersive Hyperbolic Problem

A91-40710

Philip L. Roe* and **Mohit Arora†**

The University of Michigan

Ann Arbor, Michigan

Abstract

In order to develop numerical schemes for stiff problems, we have studied a model of relaxing heat flow. To isolate those errors unavoidably associated with discretization, a method of characteristics is developed, containing three free parameters depending on the stiffness ratio. It is shown that such 'decoupled' schemes do not take into account the interaction between the wave families and hence result in incorrect wavespeeds. We also demonstrate that schemes can differ by up to two orders of magnitude in their rms errors even while maintaining second order accuracy. Next, we develop 'coupled' schemes which account for the interactions, and here we obtain two additional free parameters. We present numerical results for several decoupled and coupled schemes.

1 Introduction

In the real-life problem of attempting to solve the reactive flow equations, we often have a so-called 'stiff' problem. The flow equations are constrained to a maximum time-step by the CFL condition. Unfortunately, such large time-steps may be unacceptable for the chemical reactions. We are usually left with two choices - split the chemistry from the flow for each time step, or use the time-step dictated by the chemistry to solve the entire problem. The former reduces the credibility of the results, while the latter is prohibitively expensive computationally for obvious reasons.

It was this impasse that motivated the present work. Instead of tackling the full set of reactive flow equations right off, a simple model was derived. We expected valuable insight into the real problem since its dispersive wave characteristics are akin to those of a reactive flow with the added advantages of minimal computational cost and greatly simplified analysis. We started with the conservation of energy in a uniform conducting rod with heat flow. Instead of using Fourier's Law of Heat Conduction, which would lead to the parabolic heat equation, we use a simple model of heat conduction that has a relaxation time τ, in which information propagates at a finite speed. The result is what we call the *Hyperbolic Heat Equations*. $\tau = 0, \infty$ give us the extrema: in the first case, we have Fourier's Law with an infinite propagation speed, and in the second case, we have no propagation of information. These relations are examined using dispersion analysis, and a transformation to characteristic coordinates gives us the characteristic equations and jump relations.

We now sought to isolate the effect of stiffness on the quality of the numerical solution. We decided to use the Method of Characteristics, which is exact for linear problems without source terms, so that numerical difficulties would arise *only* due to the presence of the stiff source terms. A straightforward discretization results in the appearance of a 'stiffness factor' k in a natural manner. Due to this factor, we expected problems for $k > 1$, as some terms would change sign in this simple discretization. Another scheme we tried out was a simple one used in practice - symmetric operator splitting. Here, no terms change sign, but only the frozen wavespeeds are allowed for.

Our initial hypothesis was that since the source term prevents the characteristic equations from being integrated exactly, success, if achievable, would come from finding the best approximate quadrature. To this end, we rewrote the Method of Characteristics with three free parameters, depending on k alone, and sought to determine these by various heuristic arguments, making numerical trials of the resulting schemes. Our plan was to identify the successful heuristics, and then apply them to more complex sets of equations. Constraints on the parameters were derived from discrete dispersion relationships, discrete eigenvectors, local truncation errors, a modified conservation as well as a decoupling condition. These constraints are found to be consistent for small k but to suggest contradictory design criteria for large k. We ran tests on the various schemes varying k. Remarkably, our results show that the errors from various equally plausible characteristic schemes can eas-

*Professor, Aerospace Engineering

†Doctoral Pre-candidate, Aerospace Engineering

ily vary by two to three orders of magnitude, although all schemes retain second order convergence.

During this stage of the research, we were constantly surprised that our efforts failed to improve significantly or consistently on our first, straightforward, implementation. This eventually led us to discard the first hypothesis and to start afresh, beginning with the exact, analytic, solution to the initial-value problem. This represents the solution at a point in terms of integrals along the initial line. The integrands are composed of the Riemann function, Ω, and $u(x)$, where u may be either of q or θ. We utilize a polynomial approximation to $u(x)$ keeping terms up to second order in x, and the resulting integrals can be evaluated after some algebra. The resulting scheme contains a particular implementation of the Method of Characteristics as its leading terms, but includes additional terms that arise from coupling between the wave families. To evaluate these terms, the stencil needs to be modified to include the central point. The additional terms are small, being of third order in the stiffness factor k, but their inclusion gives results far superior to any of the uncoupled schemes, being four to five orders better than the rest of the pack for small k and about two orders better for large k. In addition, it shows a consistent third order convergence, meaning that the errors are $O(\Delta x^3)$ for any value of the parameter k. In fact, for large values of k, the coupling terms are no longer small, and the numerical scheme, like the differential problem, loses its hyperbolic character, and takes on a more parabolic appearance. With hindsight, this now appears to be essential behaviour for any numerical scheme that can cope with wave propagation in the presence of rapid reaction. We also show how greatly improved accuracy can be achieved without the benefit of knowing an exact solution.

2 A Model Equation For Dispersive Waves

We need a problem simple enough to permit detailed analysis, and carrying some physical meaning to help in understanding the results. The problem that has been chosen leads to a 2 x 2 system of equations. It has dispersive wave properties resembling those of a reactive flow, although no reaction is actually involved.

2.1 Derivation of Governing Equations

Consider the flow of heat in a uniform conducting bar. Conservation of energy can be stated as

$$\theta_t + \frac{1}{k} q_x = 0 \tag{1}$$

where θ = temperature, q = heat flow per unit area and k = heat capacity per unit volume.

Usually one now invokes Fourier's Law, that heat flow is proportional to the temperature gradient

$$q = -c\theta_x \tag{2}$$

to obtain the heat equation

$$\theta_t = \frac{c}{k}\theta_{xx} \tag{3}$$

This is, of course, the prototype of all parabolic partial differential equations, in which information propagates with infinite speed. To avoid this unrealistic result, alternative models are sometimes adopted [1], of which the simplest is to replace Equation 2 with

$$\tau q_t + c\theta_x = -q \tag{4}$$

where τ is a relaxation time. The pair of Equations 1 and 4 form a non-homogeneous hyperbolic system for which the characteristic speeds are given by $(\frac{c}{\tau k})^{\frac{1}{2}}$. For simplicity, we will adopt units in which both c and k have the value 1.0, leading to the system

$$\theta_t + q_x = 0 \tag{5}$$
$$\tau q_t + \theta_x = -q \tag{6}$$

which we will call the *Hyperbolic Heat Equations.*

2.2 Dispersion Analysis

To see the dispersive character of Equations 5 and 6, consider solutions of the form

$$\begin{pmatrix} \theta \\ q \end{pmatrix} = Re\left[\begin{pmatrix} T \\ Q \end{pmatrix} \exp[i(\omega t - \xi x)]\right] \tag{7}$$

Substituting Equation 7 into Equations 5 and 6 gives

$$i\omega T - i\xi Q = 0 \tag{8}$$
$$\tau i\omega Q - i\xi T + Q = 0 \tag{9}$$

and these equations can be solved for T and Q only if

$$\tau\omega^2 - \xi^2 = i\omega \tag{10}$$

which is the dispersion relationship for Equations 5 and 6. For an initial-value problem, ξ is a real wavenumber, and ω may be written as

$$\omega = \omega_R + i\omega_I \tag{11}$$

where ω_R is a frequency, and ω_I is a damping ratio. Substituting Equation 11 into Equation 10 gives the pair of equations

$$\omega_R(1 - 2\tau\omega_I) = 0 \tag{12}$$
$${\omega_R}^2 - {\omega_I}^2 = \frac{\xi^2 - \omega_I}{\tau} \tag{13}$$

If $\omega_R \neq 0$, then from Equation 12

$$\omega_I = \frac{1}{2\tau} \tag{14}$$

and from Equation 13,

$$\omega_R = \left(\frac{\xi^2}{\tau} - \frac{1}{4\tau^2}\right)^{\frac{1}{2}} \tag{15}$$

The quantity (ω_R/ξ) is a wavespeed, which we call $a(\xi)$. Then

$$a(\xi) = \tau^{-\frac{1}{2}}\left(1 - \frac{1}{4\tau\xi^2}\right)^{\frac{1}{2}} \tag{16}$$

For very high wavenumbers ξ, the propagation speed is the characteristic speed $\tau^{-\frac{1}{2}}$, which could also be called the frozen wavespeed. For lower wavenumbers, the propagation speed is reduced (Figure 1[upper]) becoming zero when $\xi = \frac{1}{2}\tau^{-\frac{1}{2}}$, that is, the equilibrium wavespeed vanishes. For all wavenumbers in the range $[\frac{1}{2}\tau^{-\frac{1}{2}}, \infty]$, the waves are damped like $e^{-\frac{t}{2\tau}}$.

For wavenumbers less than $\frac{1}{2}\tau^{-\frac{1}{2}}$, we have $\omega_R = 0$, and the waves do not propagate. After the typical time $t = \tau$, they are damped like $e^{-\omega_I \tau}$, with

$$\omega_I \tau = \frac{1}{2}\left[1 \pm \left(1 - 4\xi^2\tau\right)^{\frac{1}{2}}\right] \tag{17}$$

When $\xi = 0$, the solution does not depend on x, and the problem reduces to $\theta_t = 0$, $\tau q_t + q = 0$. Since these have solutions corresponding to $\omega_I \tau = 0, 1$ respectively, both branches of Equation 17 are relevant. The upper branch makes second-order contact with the dispersion relationship for the regular heat equation, which is

$$\omega_I \tau = \xi^2 \tau \tag{18}$$

shown as a dotted line in Figure 1[lower].

2.3 Characteristic and Jump Relationships

Introduce characteristic coordinates ξ,η defined by

$$\xi = t + \tau^{\frac{1}{2}} x \tag{19}$$

$$\eta = t - \tau^{\frac{1}{2}} x \tag{20}$$

then Equations 5 and 6 transform to

$$\theta_\xi + \tau^{\frac{1}{2}}\left(q_\xi + \frac{q}{2\tau}\right) = 0 \tag{21}$$

$$\theta_\eta - \tau^{\frac{1}{2}}\left(q_\eta + \frac{q}{2\tau}\right) = 0 \tag{22}$$

which are the characteristic equations. Unfortunately, it is not possible to integrate these equations and obtain Riemann invariants, as can be done with linear homogeneous problems. Thus, a numerical method of characteristics is no longer an exact method.

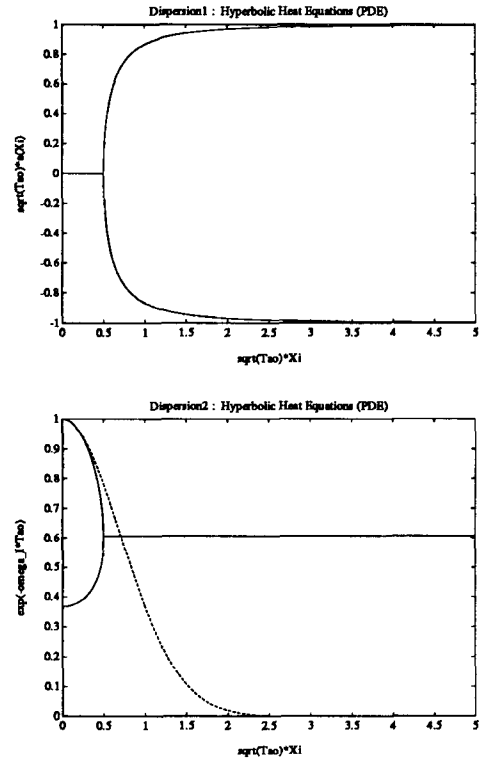

Figure 1: Analytic Dispersion Diagrams for the Hyperbolic and Parabolic Heat Equations

As usual, the solution will admit discontinuities that lie along characteristic paths. It is easy to show that the jump relationships are those of the homogeneous problem, i.e., across a jump lying in the ξ-direction

$$\Delta\theta = \tau^{\frac{1}{2}}\Delta q \tag{23}$$

and across a jump lying in the η-direction

$$\Delta\theta = -\tau^{\frac{1}{2}}\Delta q \tag{24}$$

3 A Riemann Problem for the Hyperbolic Heat Equations

A natural problem to pose in connection with the hyperbolic model of heat conduction is that of two semi-infinite rods, having temperatures θ_L, θ_R, brought into contact at $t = 0$. The solution will be of the form shown in Figure 2.

The problem is to find θ, q, in the region POQ. There is an analytic solution for q, which is (see article 12 of [2])

$$\begin{aligned} q(\xi,\eta) &= \left(\frac{\theta_L - \theta_R}{2\tau^{\frac{1}{2}}}\right)\exp\left(-\frac{\xi+\eta}{4\tau}\right) I_0\left(\sqrt{\frac{\xi\eta}{4\tau^2}}\right) \\ &= \left(\frac{\theta_L - \theta_R}{2\tau^{\frac{1}{2}}}\right)\exp\left(-\frac{t}{2\tau}\right) I_0\left(\sqrt{\frac{t^2 - \tau x^2}{4\tau^2}}\right) \end{aligned} \tag{25}$$

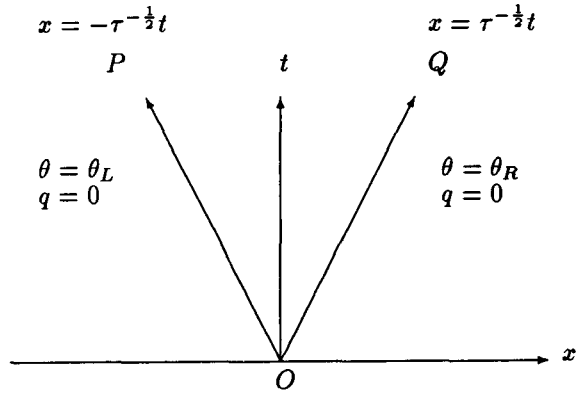

Figure 2: Schematic of the problem

where I_0 is the modified Bessel function of order zero. This can be written in the similarity form

$$\frac{\tau^{\frac{1}{2}}q}{\Delta\theta} = fn\left(\frac{\xi}{\tau}, \frac{\eta}{\tau}\right) \tag{26}$$

showing that solutions for different τ are not really independent, but affinely related.

There appears to be no closed-form solution for θ, but a solution that is sufficiently accurate for testing the numerical results can be found by numerically integrating Equation 6, knowing q and q_t analytically, using Gaussian quadrature formulae.

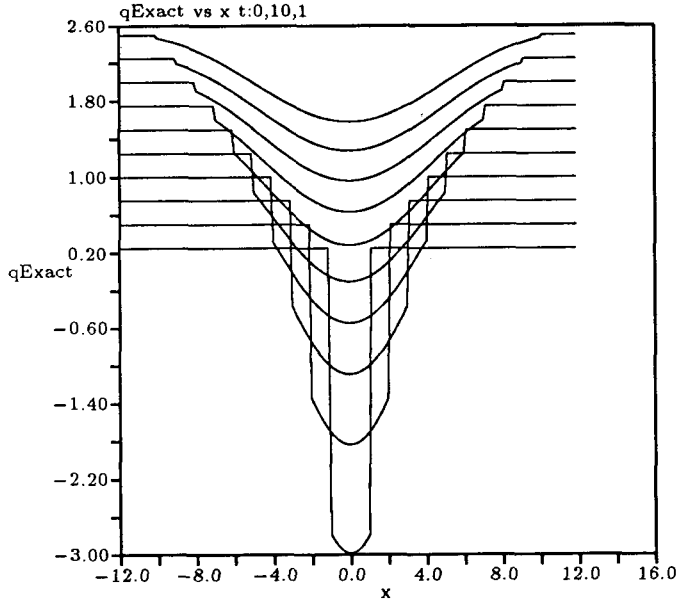

Figure 3: Exact solution to the Riemann Problem for the heat flow q

The character of the solution can be appreciated from Figure 3. For t/τ small, the solution is typically hyperbolic and strongly discontinuous, but the jumps in the solution decay like $\exp(-\frac{t}{2\tau})$ (which is also the rate at which high wavenumbers decay).

As time increases, the solution assumes a more typically parabolic character. The region of space within which significant variations occur grows, not linearly, but like $t^{\frac{1}{2}}$. In fact, for large times, the expression given by Equation 25 simplifies to

$$q(x,t) = \left(\frac{\theta_L - \theta_R}{2\sqrt{\pi t}}\right) \exp\left(-\frac{x^2}{4t}\right) \tag{27}$$

which is the classical fundamental solution to the heat equation.

4 A Numerical Method of Characteristics

In this section, we develop and analyse the numerical method of characteristics for the hyperbolic heat equations. We begin with a simple treatment that apparently does not take into account the potential stiffness of the problem.

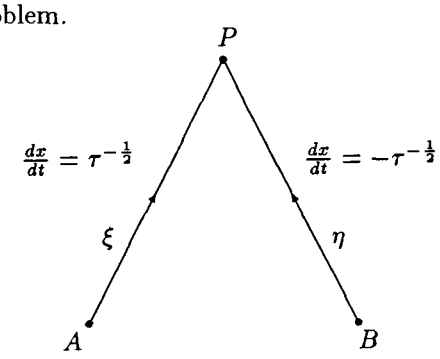

Figure 4: Stencil for the Method of Characteristics

Given, as in Figure 4, a point P and two characteristic lines PA and PB, we make the obvious discretization of Equations 21 and 22 as

$$(\theta_P - \theta_A) + \tau^{\frac{1}{2}}\left[q_P - q_A + \frac{\Delta t}{2\tau}(q_P + q_A)\right] = 0 \tag{28}$$

$$(\theta_P - \theta_B) - \tau^{\frac{1}{2}}\left[q_P - q_B + \frac{\Delta t}{2\tau}(q_P + q_B)\right] = 0 \tag{29}$$

Solving these equations, we have

$$\theta_P = \left(\frac{\theta_A + \theta_B}{2}\right) + \frac{\tau^{\frac{1}{2}}}{2}(1-k)(q_A - q_B) \tag{30}$$

$$q_P = \left(\frac{1-k}{1+k}\right)\left(\frac{q_A + q_B}{2}\right) + \frac{\tau^{-\frac{1}{2}}}{2(1+k)}(\theta_A - \theta_B) \tag{31}$$

where we have written

$$k = \frac{1}{2}\frac{\Delta t}{\tau} \tag{32}$$

Henceforward, we refer to k as the stiffness parameter. Because of the geometry of the characteristic mesh,

note that we also have

$$k = \frac{1}{2}\frac{\Delta x}{\tau^{\frac{1}{2}}} \tag{33}$$

Now let us rewrite Equations 30 and 31 as follows:

$$\theta_P = \left(\frac{\theta_A + \theta_B}{2}\right) + \frac{\tau^{\frac{1}{2}}}{2} X(k)(q_A - q_B) \tag{34}$$

$$q_P = Z(k)\left(\frac{q_A + q_B}{2}\right) + \frac{\tau^{-\frac{1}{2}}}{2} Y(k)(\theta_A - \theta_B) \tag{35}$$

Here, we have introduced three general functions of k which appear as coefficients in Equations 34 and 35. This is the general solution to the Hyperbolic Heat Equations by the Method of Characteristics. For our simple discretization which we call version 0, we have

$$X = 1 - k \tag{36}$$

$$Y = (1+k)^{-1} \tag{37}$$

$$Z = (1-k)(1+k)^{-1} \tag{38}$$

4.1 A Practical Scheme - Operator Splitting

We break our problem solution into two parts. In one, we solve the homogeneous problem

$$\theta_t + q_x = 0 \tag{39}$$

$$\tau q_t + \theta_x = 0 \tag{40}$$

In the other, we solve for the damping due to the source term as

$$q_i^{n+1} = q_i^n \exp^{t/\tau} \tag{41}$$

Let us call the damping operation L_1 and the solution to the homogeneous problem by the Method of Characteristics L_2. To get second order accuracy, we must use one of the sequence of operations $L_1L_2L_2L_1$ or $L_2L_1L_1L_2$ [3]. For the sequence $L_1L_2L_2L_1$

$$\theta_i^{n+\frac{1}{4}} = \theta_i^n \tag{42}$$

$$q_i^{n+\frac{1}{4}} = q_i^n e^{-k} \tag{43}$$

$$\theta_i^{n+\frac{3}{4}} = \left[\left(\frac{\theta_{i-1} + \theta_{i+1}}{2}\right) + \tau^{\frac{1}{2}}\left(\frac{q_{i-1} - q_{i+1}}{2}\right)\right]^{n+\frac{1}{4}} \tag{44}$$

$$q_i^{n+\frac{3}{4}} = \left[\left(\frac{q_{i-1} + q_{i+1}}{2}\right) + \tau^{-\frac{1}{2}}\left(\frac{\theta_{i-1} - \theta_{i+1}}{2}\right)\right]^{n+\frac{1}{4}} \tag{45}$$

$$\theta_i^{n+1} = \theta_i^{n+\frac{3}{4}} \tag{46}$$

$$q_i^{n+1} = q_i^{n+\frac{3}{4}} e^{-k} \tag{47}$$

In short, we get Equations 34 and 35 with

$$X(k) = e^{-k} \tag{48}$$

$$Y(k) = e^{-k} \tag{49}$$

$$Z(k) = e^{-2k} \tag{50}$$

which we will refer to as version 9.

4.2 Some Numerical Results

In Figure 5 we plot on log-log scales the rms error in q (at $\frac{t}{\tau} = 3, 6, 10, 30, 60, 100, 300, 600, 1000$) versus k for the method of characteristics version 0 (the straightforward discretization), applied to the Riemann problem described in Section 3. In Figure 6, the exercise is repeated for version 9 (operator splitting). As boundary conditions we have supplied the analytical solution along both limiting characteristics. Thus we do not attempt to capture the discontinuities, and our tests relate purely to the smooth part of the solution.

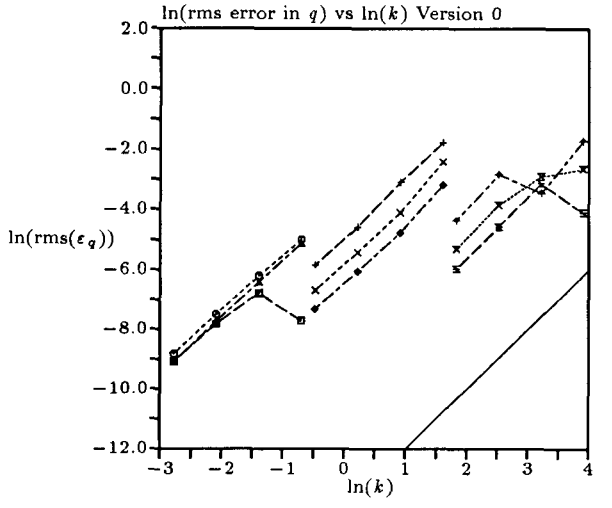

Figure 5: rms error in q vs k for version 0

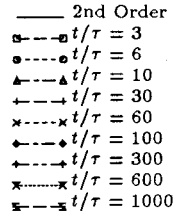

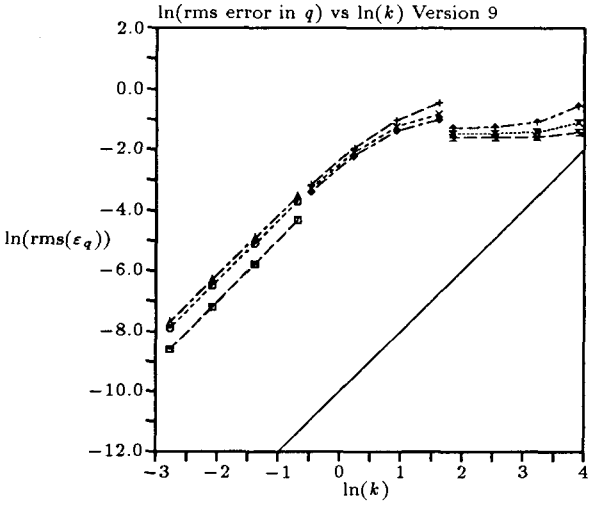

Figure 6: rms error in q vs k for version 9

In Figures 7 and 8, we make similar plots for errors in θ (obtained by comparison with an accurate solution obtained by integration of Equation 6 using the Gaussian quadrature formulae). In all cases, the errors are normalized so that $ln(\varepsilon) = 0$ indicates an error of the same size as the solution.

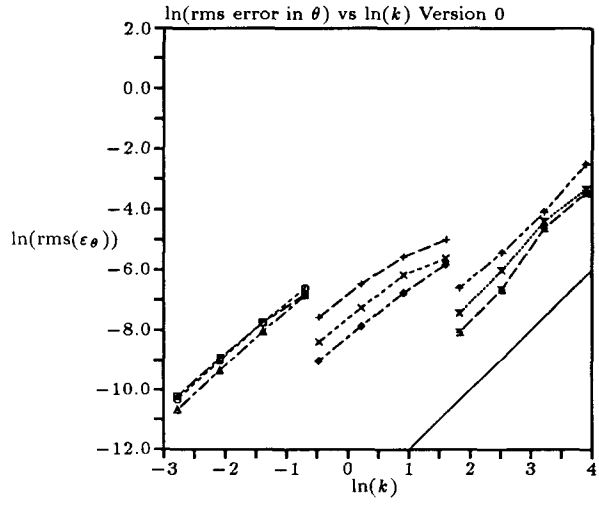

Figure 7: rms error in θ vs k for version 0

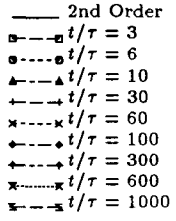

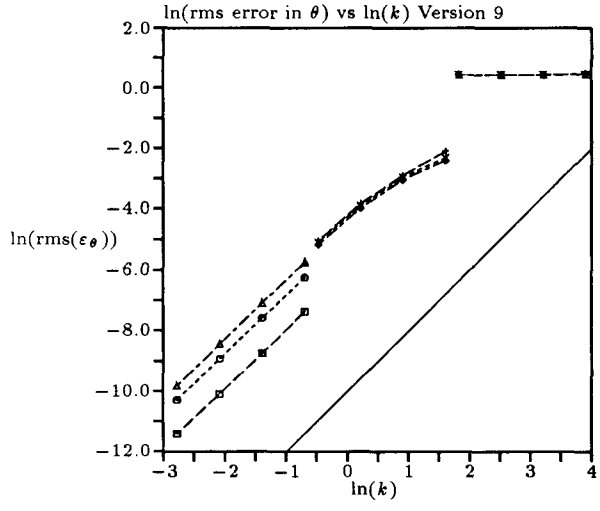

Figure 8: rms error in θ vs k for version 9

We see that all our solutions are quite consistently giving slopes of two (as seen by comparison with the solid line), indicating second-order accuracy, for k less than about 2.

Surprisingly enough, although Version 0 looks as though it should break down for $k > 1$, it continues to give useful answers for values of k up to about 25 or so, whereas Version 9, which contains no obvious signs of trouble, does not produce useful answers beyond $k \simeq 2$. To improve on these methods, we looked for combinations of $X(k)$, $Y(k)$, and $Z(k)$ that would enforce a variety of apparently desirable properties. Some of these were derived from the dispersion relationship of the discrete equations, which is

$$\exp(i\omega\Delta t) = \frac{(1+Z)\cos(\xi\Delta x)}{2} \pm \frac{[(1-Z)^2\cos^2(\xi\Delta x) - 4XY\sin^2(\xi\Delta x)]^{\frac{1}{2}}}{2} \tag{51}$$

We list below some of the constraints that were tried, together with the properties that each bestows.

1) This condition ensures that
   - (a) all propagating waves have the same damping ratio
   - (b) the scheme is derivable from some pair of characteristic equations

$$X(k)Y(k) = Z(k) \tag{52}$$

2) This condition
   - (a) eliminates the leading error term from the Local Truncation Error of the q-equation
   - (b) ensures 'conservation' of the quantity $e^{\frac{t}{\tau}}q$
   - (c) ensures correct damping at low wavenumbers

$$Z(k) = e^{-2k} \tag{53}$$

3) This condition ensures that the eigenvectors of the discrete equation match those of the analytic equation

$$\frac{2kX(k)}{1 - X(k)Y(k)} = 1 \tag{54}$$

4) This condition ensures the correct separation between propagating and non-propagating waves

$$\frac{(1-Z(k))^2}{4X(k)Y(k)} = \tan^2(k) \tag{55}$$

5) This condition ensures correct damping for the highest wavenumbers

$$X(k)Y(k) = e^{-2k} \tag{56}$$

It is possible to satisfy all of these constraints to within an error of $O(k^2)$. However, by choosing to satisfy one or more of them exactly, we generate a variety of schemes with different properties.

A sample plot of several such decoupled schemes is given in Figure 9, where we plot the error in θ versus k at $\frac{t}{\tau} = 10$ for some of these schemes. This demonstrates the interesting fact that schemes derived from sound fundamentals all give slopes of two (as indicated by the solid line), but exhibit two orders of magnitude difference between the best and worst results.

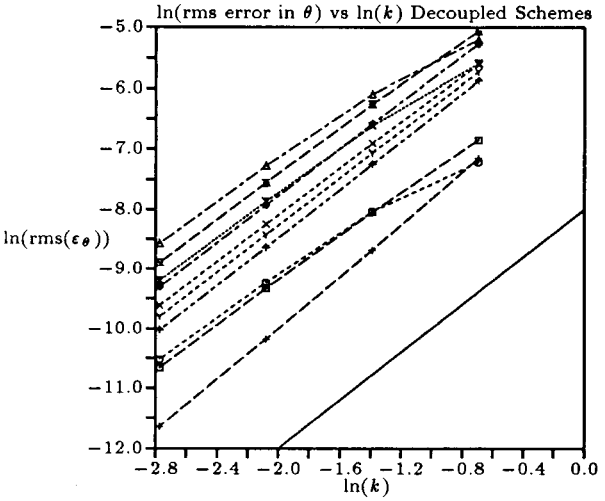

Figure 9: rms error in θ vs k for several Decoupled Schemes at $t/\tau = 10$

4.3 A New Direction

Our constraint relations provided consistent design criteria for small k but contradicted each other for large k. Our results have shown widely differing errors, but we also found that we were never really doing much better than the simple discretization. These observations motivated us to reject our initial hypothesis that there is a scheme which has desirable characteristics for large k, which can be put together from constraints arrived at by heuristic arguments. We then began anew with the exact, analytic solution to the Initial-Value Problem at hand. This led us to the new hypothesis that for any scheme to posess the ability to cope with wave propagation in the presence of rapid reactions, there must exist a coupling between the characteristics to account for the change in wavespeeds. This effect should also be more pronounced at large values of the stiffness parameter k. In order to account for the coupling, our computational stencil gets modified and now includes the middle point. The resulting scheme we call the *Coupled Method of Characteristics*, which is what we focus on next.

5 The Coupled Method of Characteristics

In this section, we shall derive the general equations for the Coupled Method of Characteristics and the design parameters that define them, analyse them - analytically, to the extent possible, and numerically - and then present results from some tests run.

We begin with the stencil shown in Figure 10

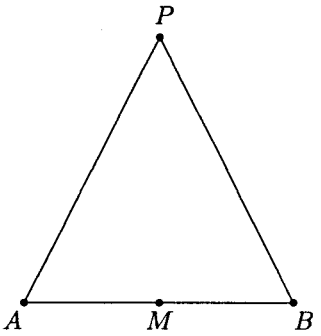

Figure 10: Stencil for the Coupled Method of Characteristics

By an extension of the analysis given in [2], we can obtain

$$\theta_P = \frac{1}{2}e^{-k}(\theta_A+\theta_B)+\frac{\tau^{\frac{1}{2}}}{2}\int_A^B(\frac{\Omega}{\tau}-\Omega_t)\theta dx-\frac{\tau^{\frac{1}{2}}}{2}\int_A^B \Omega q_x dx \quad (57)$$

$$q_P = \frac{1}{2}e^{-k}(q_A+q_B)-\frac{\tau^{\frac{1}{2}}}{2}\int_A^B \Omega_t q dx-\frac{\tau^{-\frac{1}{2}}}{2}\int_A^B \Omega\theta_x dx \quad (58)$$

where Ω is the Riemann function

$$\Omega(\xi,\eta) = exp\left(\frac{\xi-\xi_1+\eta-\eta_1}{4\tau}\right) I_0\left(\sqrt{\frac{(\xi-\xi_1)(\eta-\eta_1)}{4\tau^2}}\right) \quad (59)$$

To create a numerical method we have to evaluate the integrals. In these, the functions, Ω and Ω_t are of course known exactly, but the functions θ, q, θ_x and q_x have to be approximated using the available information. We will represent them as polynomials as follows

$$\begin{aligned} u(x) &= \frac{1}{2}(u_A+u_B)+\frac{x}{4k\tau^{\frac{1}{2}}}(u_B-u_A)+ \\ &\quad \frac{x^2-4k^2\tau}{8k^2\tau}(u_A-2u_M+u_B) \\ &\quad +O(\Delta x^3) \end{aligned} \quad (60)$$

$$\begin{aligned} u_x(x) &= \frac{(u_B-u_A)}{4k\tau^{\frac{1}{2}}}+\frac{x}{4k^2\tau}(u_A-2u_M+u_B) \\ &\quad +O(\Delta x^2) \end{aligned} \quad (61)$$

Note that since Ω and Ω_t are even functions, only the even parts of u and u_x will contribute to the integrals. The required integrals are of the form

$$I_P = \int_A^B x^P \Omega dx \quad (62)$$

$$J_P = \int_A^B x^P \Omega_t dx \quad (63)$$

These can be evaluated in terms of Bessel functions of half-integer order and are expressible in terms of exponentials and polynomials [4] leading to

$$\theta_P = \frac{1}{2}(\theta_A + \theta_B) + \frac{\tau^{\frac{1}{2}}}{4k}(1 - e^{-2k})(q_A - q_B) + \frac{1}{4k^2}(e^{-2k} - 1 + 2k - 2k^2)(\theta_A - 2\theta_M + \theta_B) + O(\tau^{\frac{1}{2}}\Delta_x^3)q_{xxx} \quad (64)$$

$$q_P = \frac{e^{-2k}}{2}(q_A + q_B) + \frac{\tau^{-\frac{1}{2}}}{4k}(1 - e^{-2k})(\theta_A - \theta_B) - \frac{1}{4k^2}[e^{-2k}(1 + 2k + 2k^2) - 1](q_A - 2q_M + q_B) + O(\tau^{-\frac{1}{2}}\Delta_x^3)\theta_{xxx} \quad (65)$$

In each of the above equations, the terms in the top line make reference only to the values at P, A and B, and give the appearance of a Method of Characteristics solution. However, the truncated equations cannot be decomposed into a pair of characteristic equations because they fail to satisfy Equation 52. Thus, some coupling of the characteristics is already involved.

The second difference terms are in each case of order $k\Delta x^2$, and hence negligible for small k, but need to be considered for large k. We will refer to Equations 64 and 65 as the Optimum scheme, because it gives the closest approximation possible to the exact solution (Equations 57 and 58) with the data available in Figure 10.

We can rewrite Equations 64 and 65 in the form

$$\theta_P = R_\theta(k)\frac{1}{2}(\theta_A + \theta_B) + S_\theta(k)\frac{\tau^{\frac{1}{2}}}{2}(q_A - q_B) + T_\theta(k)(\theta_A - 2\theta_M + \theta_B) \quad (66)$$

$$q_P = R_q(k)\frac{1}{2}(q_A + q_B) + S_q(k)\frac{\tau^{-\frac{1}{2}}}{2}(\theta_A - \theta_B) + T_q(k)(q_A - 2q_M + q_B) \quad (67)$$

The coefficients R_θ, S_θ, T_θ, R_q, S_q and T_q are tabulated in Table 1. Their polynomial expansions for small k are given in Table 2 while the asymptotic behaviour of the coefficients is tabulated in Table 3.

5.1 Some Numerical Results

In Figures 11 and 12, we plot the error in q and θ for the Coupled Method of Characteristics exactly as we had done earlier in Figures 5 and 7. Here we consistently see a slope of three, indicating third order accuracy.

6 Some Simple Coupled Schemes

In Section 5, we achieved exceptionally good results which reenforced our hypothesis that a correct scheme must account for the coupling between waves, and hence must make use of the middle point in our stencil. This can be done using a variety of integration schemes. In each of these schemes, we use the stencil given in Figure 13.

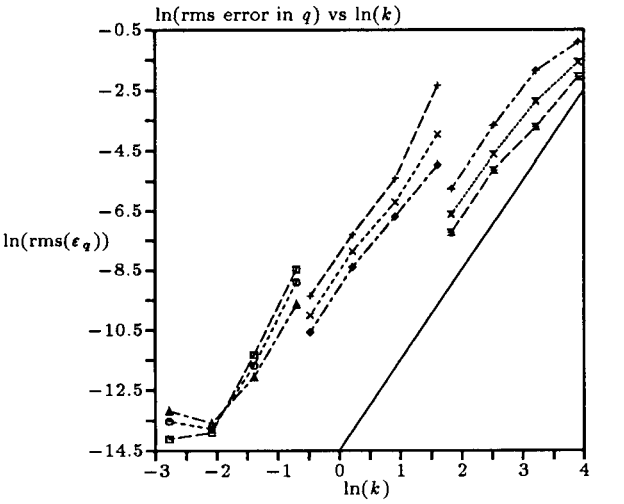

Figure 11: rms error in q vs k for the Optimum scheme

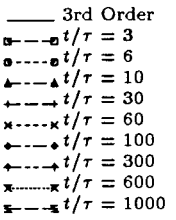

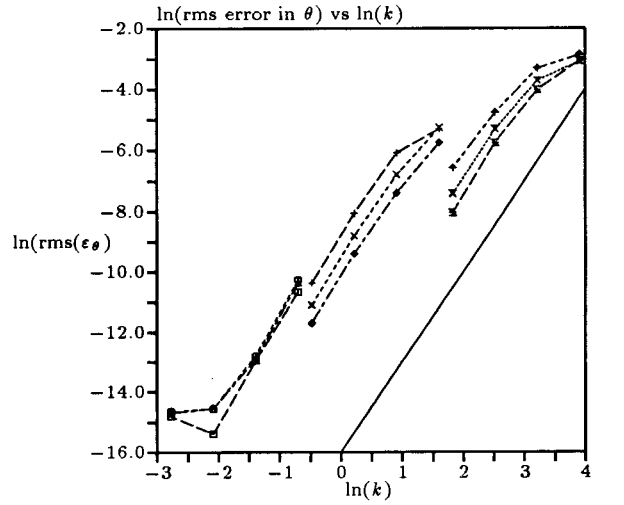

Figure 12: rms error in θ vs k for the Optimum scheme

We use the simple method of characteristics on AMF and MBG to obtain q_F and q_G. Now, we integrate the characteristic equations (Equations 21 and 22) using the simple method of characteristics, modified to integrate the source term using the information now available at F and G. Substitution of the expressions for

Version Definition for Coupled Schemes

Version	$R_\theta(k)$	$S_\theta(k)$	$T_\theta(k)$	$R_q(k)$	$S_q(k)$	$T_q(k)$
Optimum	1	$\frac{1-e^{-2k}}{2k}$	$\frac{e^{-2k}-1+2k-2k^2}{4k^2}$	e^{-2k}	$\frac{1-e^{-2k}}{2k}$	$\frac{1-e^{-2k}(1+2k+2k^2)}{4k^2}$
Simpson	1	$\frac{6-3k+k^2}{3(2+k)}$	$-\frac{2k}{3(2+k)}$	$\frac{6-7k+3k^2}{6+5k+k^2}$	$\frac{6-k}{6+5k+k^2}$	$\frac{k(2-k)}{6+5k+k^2}$
Trapezium	1	$\frac{2-k}{2+k}$	$-\frac{k}{2(2+k)}$	$\left(\frac{2-k}{2+k}\right)^2$	$\left(\frac{2}{2+k}\right)^2$	$\frac{k(2-k)}{2(2+k)^2}$
Pade	1	$\frac{3+0.1k^6}{3+3k+k^2+0.2k^7}$	$-\frac{k(1+0.295k)}{3+0.6k(4+k)}$	e^{-2k}	$\frac{3+0.1k^6}{3+3k+k^2+0.2k^7}$	$\frac{k(\frac{1}{3}-0.1402k+0.01k^5)}{1+k(1.0794+0.4191k+0.04k^7)}$
MidPoint	1	$\frac{2-k+k^2}{2+k}$	$-\frac{k}{2+k}$	$\frac{2-3k+2k^2}{2+k}$	$\frac{2-k}{2+k}$	$\frac{k(2-k)}{2(2+k)}$

Table 1: Coefficients R_θ, S_θ, T_θ, R_q, S_q and T_q for the Coupled Schemes

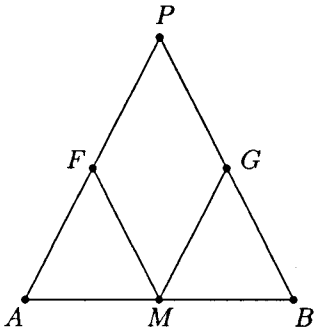

Figure 13: Stencil for the Simple Coupled Schemes

q_F and q_G in the resulting equations provides explicit expressions for θ_P and q_P. Our first attempt was to use Simpson's Rule, followed by even simpler integration schemes - the Trapezoidal Rule and the Midpoint Rule. Finally, we try to construct a scheme using only asymptotic information and the Padé approximation. These schemes of course no longer rely on knowledge of an exact solution. We derive the design parameters for each of these variants next, followed by a sampling of our results for the Coupled Schemes in Figure 14.

6.1 The Coupled Scheme via Simpson's Rule

A straightforward application of the method of characteristics to AMF and MBG using version 0 results in

$$q_F = \left(\frac{2-k}{2+k}\right)\left(\frac{q_A+q_M}{2}\right)+\left(\frac{\tau^{-\frac{1}{2}}}{2+k}\right)(\theta_A-\theta_M) \quad (68)$$

$$q_G = \left(\frac{2-k}{2+k}\right)\left(\frac{q_M+q_B}{2}\right)+\left(\frac{\tau^{-\frac{1}{2}}}{2+k}\right)(\theta_M-\theta_B) \quad (69)$$

Now, we integrate the characteristic equations, (Equations 21 and 22) on the stencil ABP to get

$$(\theta_P-\theta_A)+\tau^{\frac{1}{2}}\left[q_P-q_A+\frac{\Delta t}{6\tau}(q_A+4q_F+q_P)\right]=0 \quad (70)$$

$$(\theta_P-\theta_B)-\tau^{\frac{1}{2}}\left[q_P-q_B+\frac{\Delta t}{6\tau}(q_B+4q_G+q_P)\right]=0 \quad (71)$$

where we have used Simpson's Rule to evaluate the source terms. We can solve for θ_P and q_P in terms of values at A, B, F and G. On substitution of the expressions for q_F and q_G from Equations 68 and 69 into the above equations, we get explicit expressions for θ_P and q_P which give coefficients R_θ, S_θ, T_θ, R_q, S_q and T_q as tabulated in Table 1. The polynomial expansion of the coefficients for small k is given in Table 2 while their asymptotic behaviour is in Table 3.

Looking at these, we expect excellent results for small k but a lot of problems for large k. This is evidenced by our numerical results, a sample of which may be seen from Figure 14.

6.2 The Coupled Scheme via the Trapezium Rule

All that changes if we use the Trapezium Rule as opposed to Simpson's Rule is that the integrated characteristic equations now read

$$(\theta_P-\theta_A)+\tau^{\frac{1}{2}}\left[q_P-q_A+\frac{\Delta t}{4\tau}(q_A+2q_F+q_P)\right]=0 \quad (72)$$

$$(\theta_P-\theta_B)-\tau^{\frac{1}{2}}\left[q_P-q_B+\frac{\Delta t}{4\tau}(q_B+2q_G+q_P)\right]=0 \quad (73)$$

Once again, we can solve for θ_P and q_P to get the coefficients R_θ, S_θ, T_θ, R_q, S_q and T_q, their polynomial expansions for small k and their asymptotic behaviour, as tabulated in Tables 1, 2 and 3 respectively.

		Polynomial Expansion				
Coeft	*Scheme*	1	k	k^2	k^3	k^4
R_θ	*Optimum*	1	0	0	0	0
	Simpson	1	0	0	0	0
	Trapezium	1	0	0	0	0
	Pade	1	0	0	0	0
	MidPoint	1	0	0	0	0
S_θ	*Optimum*	1	-1	$\frac{2}{3}$	$-\frac{1}{3}$	$\frac{2}{15}$
	Simpson	1	-1	$\frac{2}{3}$	$-\frac{1}{3}$	$\frac{1}{6}$
	Trapezium	1	-1	$\frac{1}{2}$	e	e
	Pade	1	-1	$\frac{2}{3}$	$-\frac{1}{3}$	$\frac{1}{9}$
	MidPoint	1	-1	1	e	e
T_θ	*Optimum*	0	$-\frac{1}{3}$	$\frac{1}{6}$	$-\frac{1}{15}$	$\frac{1}{45}$
	Simpson	0	$-\frac{1}{3}$	$\frac{1}{6}$	$-\frac{1}{12}$	e
	Trapezium	0	$-\frac{1}{4}$	e	e	e
	Pade	0	$-\frac{1}{3}$	$\frac{1}{5.941}$	e	e
	MidPoint	0	$-\frac{1}{2}$	e	e	e
R_q	*Optimum*	1	-2	2	$-\frac{4}{3}$	$\frac{2}{3}$
	Simpson	1	-2	2	$-\frac{4}{3}$	$\frac{7}{9}$
	Trapezium	1	-2	2	$-\frac{3}{2}$	e
	Pade	1	-2	2	$-\frac{4}{3}$	$\frac{2}{3}$
	MidPoint	1	-2	2	$-\frac{3}{4}$	e
S_q	*Optimum*	1	-1	$\frac{2}{3}$	$-\frac{1}{3}$	$\frac{2}{15}$
	Simpson	1	-1	$\frac{2}{3}$	$-\frac{7}{18}$	e
	Trapezium	1	-1	$\frac{3}{4}$	e	e
	Pade	1	-1	$\frac{2}{3}$	$-\frac{1}{3}$	$\frac{1}{9}$
	MidPoint	1	-1	$\frac{1}{2}$	e	e
T_q	*Optimum*	0	$\frac{1}{3}$	$-\frac{1}{2}$	$\frac{2}{5}$	$-\frac{2}{9}$
	Simpson	0	$\frac{1}{3}$	$-\frac{4}{9}$	e	e
	Trapezium	0	$\frac{1}{4}$	e	e	e
	Pade	0	$\frac{1}{3}$	$-\frac{1}{2}$	$\frac{2}{5}$	$-\frac{2}{9}$
	MidPoint	0	$\frac{1}{2}$	e	e	e

Table 2: Polynomial Expansion of the coefficients of the Coupled schemes about $k = 0$. Note that terms are retained till the 1st error term after which we use the symbol 'e'

We still expect decent results for small k, but they would obviously not be as good as the Simpson Rule integrated results. Here, too, the large k solutions are expected to be bad, but in every case, the asymptotic behaviour of the coefficients is improved, so it would be expected that for large k the solutions obtained by Trapezoidal integration would be (perhaps surprisingly) better than for integration by Simpson's Rule. This, too, is observed from our numerical experiments (Figure 14).

6.3 The Coupled Scheme via the Mid-Point Rule

Here, we use the MidPoint Rule and the integrated characteristic equations now read

$$(\theta_P - \theta_A) + \tau^{\frac{1}{2}} \left[q_P - q_A + \frac{\Delta t}{\tau} q_F \right] = 0 \qquad (74)$$

$$(\theta_P - \theta_B) - \tau^{\frac{1}{2}} \left[q_P - q_B + \frac{\Delta t}{\tau} q_G \right] = 0 \qquad (75)$$

and the solutions for θ_P and q_P give us the coefficients R_θ, S_θ, T_θ, R_q, S_q and T_q, their polynomial expansions for small k, and their asymptotic behaviour, which are tabulated in Tables 1, 2 and 3 respectively.

We find that with the midpoint rule our scheme reverts to second-order accuracy for small k, and that under asymptotic conditions the match with the optimum scheme deteriorates further (Figure 14).

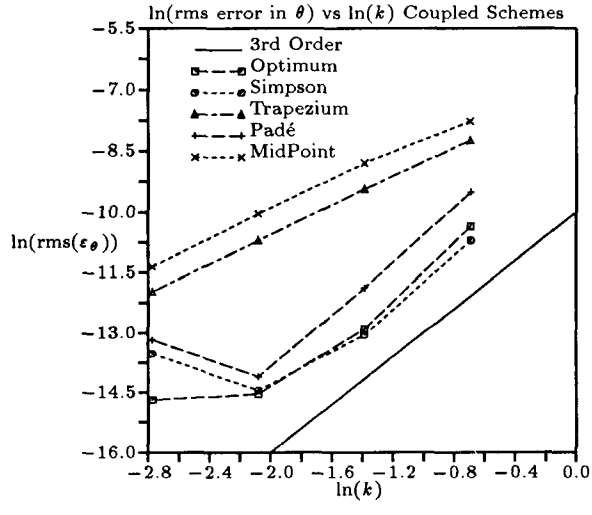

Figure 14: rms error in θ vs k for several Coupled Schemes

6.4 The Padé Approximation

In real life problems, it is unlikely that we have at our disposal an exact analytical solution. But it is very

Asymptotic Behaviour of Coupled Schemes Coefficients

Version	R_θ	S_θ	T_θ	R_q	S_q	T_q
Optimum	1	$\sim \frac{1}{2k}$	$-\frac{1}{2}$	$\sim e^{-2k}$	$\sim \frac{1}{2k}$	$\sim \frac{1}{4k^2}$
Simpson	1	$\sim \frac{1}{3}k$	$-\frac{2}{3}$	3	$\sim -\frac{1}{k}$	-1
Trapezium	1	-1	$-\frac{1}{2}$	1	$\sim \frac{4}{k^2}$	$-\frac{1}{2}$
Pade	1	$\sim \frac{1}{2k}$	-0.492	$\sim e^{-2k}$	$\sim \frac{1}{2k}$	$\sim \frac{1}{4k^2}$
MidPoint	1	$\sim k$	-1	$\sim 2k$	-1	$-\frac{k}{2}$

Table 3: Asymptotic behaviour of the coefficients for the Coupled Schemes

likely that we would have asymptotic information. In this section, we have only used the polynomial expansions for the exact solution and the asymptotic solution to create rational function approximations to the coefficients R_θ, S_θ, T_θ, R_q, S_q and T_q using the Padé approximation. We are of the opinion that such functions could be generated with a little algebra (perhaps computer assisted) for real-life problems too. The coefficients, their polynomial expansions for small k, and their asymptotic behaviour are tabulated in Tables 1, 2 and 3 respectively. And the results are very good across the entire spectrum of k as the coefficients vary smoothly with k (Figure 14). This could have tremendous potential for practical applications.

7 Conclusions and Future Work

We have shown that for the hyperbolic heat equations the decoupled method of characteristics is not desirable as it does not take into account the interaction between wave families. In addition, schemes that would appear to be equally plausible may actually differ by up to two orders of magnitude in their normalized errors. The coupled schemes we developed do account for wave interactions, and result in greatly improved accuracy. Furthermore, it has been demonstrated that such schemes can be developed even without knowledge of an exact solution. In fact, we have constructed a fairly good scheme simply using asymptotic information (a very realistic scenario).

It is our belief that lessons learned here will be transferable to more realistic problems, at least qualitatively. The next step would be to see what happens when the CFL number is no longer unity. More pragmatic schemes could be constructed, and the stencil expanded for greater accuracy. Shock capturing could be implemented with the help of limiters. It is encouraging that TVD schemes for the hyperbolic heat equations have been very successfully implemented by Yang [5], although he does not explicitly address the issue of stiffness. More realistic problems such as acoustic disturbances in a relaxing medium could be attacked. And if, as we hope, the ideas *are* transferable to more complex problems, a systematic procedure to deal with the stiffness of relaxing and reacting flow computations will have been established.

Acknowledgement

This work was supported in part by a University Consortium Agreement (NCA2-521) with NASA Ames Research Centre. The authors are grateful to Dr. Helen Yee and Dr. Steve Deiwert for their support and encouragement.

References

[1] G. Lebon and A. Cloot, "Propagation of ultrasonic sound waves in dissipative dilute gases and extended irreversible thermodynamics", *Wave Motion*, 11, pp 23-32, 1989.

[2] R. von Mises. *Mathematical Theory of Compressible Fluid Flow*, Academic Press, New York, 1958.

[3] G. Strang, "On the construction and comparison of difference schemes", *SIAM J. Num. Anal.*, 5, p 506, 1968.

[4] M. Abramowitz and I. A. Stegun (Eds.) *Handbook of Mathematical Functions*, National Bureau of Standards, 10th printing, 1972.

[5] H. Q. Yang, "Characteristic-based, high-order accurate and nonoscillatory numerical method for hyperbolic heat conduction", *Numerical Heat Transfer, Part B*, 18, pp 221-241, 1990.